International Journal of High-Rise Buildings
March 2012, Vol 1, No 1, 1-13

International Journal of
High-Rise Buildings
www.ctbuh.org

Amplitude Dependency of Damping in Buildings and Critical Tip Drift Ratio

Yukio Tamura†

School of Architecture and Wind Engineering, Tokyo Polytechnic University, Atsugi 243-0297, Japan

Abstract

The importance of appropriate use of damping evaluation techniques and points to note for accurate evaluation of damping are first discussed. Then, the variation of damping ratio with amplitude is discussed, especially in the amplitude range relevant to wind-resistant design of buildings, i.e. within the elastic limit. The general belief is that damping increases with amplitude, but it is emphasized that there is no evidence of increasing damping ratio in the very high amplitude range within the elastic limit of main frames, unless there is damage to secondary members or architectural finishings. The damping ratio rather decreases with amplitude from a certain tip drift ratio defined as "critical tip drift ratio," after all friction surfaces between primary/structural and secondary/non-structural members have been mobilized.

Keywords: Damping, Wind-induced response, Amplitude dependency, Critical tip drift ratio, Damping evaluation technique

1. Introduction

In order to accurately evaluate the responses of buildings and structures under wind, earthquake or other external excitations, their dynamic properties such as natural frequencies, mode shapes and damping ratios should be exactly known. Damping is the most important dynamic but most uncertain parameter affecting the dynamic responses of buildings and structures. This uncertainty significantly reduces the reliability of structural design for dynamic effects. For example, the C.O.V. of full-scale data has been estimated at almost 70% (Havilland, 1976). If the design value of damping ratio is set at 2% based on the mean value of full-scale data, mean $\pm \sigma$ (standard deviation) ranges from 0.6% to 3.4% (= 2% ± 1.4%). If we evaluate wind-induced acceleration responses of a tall building with almost 5.7 times difference between damping ratios (= 3.4/0.6), the acceleration responses show 2.4 times difference. Therefore, accurate evaluation of design damping ratio is a pressing need for tall building design. Another important suggestion on application of damping devices can be derived from this fact. If we could assure additional damping, say 4%, by applying a damping device, the total damping ratio in the building would range from 4.6% to 7.4%, i.e., the difference would be only 1.6 times, and the difference between the resultant acceleration responses would be only 1.3 times.

Unlike seismic excitations, wind excitations last for a long period, e.g. a few hours, and induced building responses are composed of a static component, a quasi-static component, and a resonant component, as shown in Fig. 1. If the response level exceeds the elastic limit, the natural frequency shifts to a lower frequency due to softening phenomena in the plastic region (Tamura et al., 2001; Tamura, 2009). This natural frequency shift results in an increase in the corresponding wind force spectrum, and can potentially increase the resonant component. The static component also shows some interesting behaviors such as a sudden increase in the along-wind direction (Tsujita et al., 1997; Tamura et al., 2001). There are various uncertainties in the characteristics of wind-induced responses of a building in the plastic region due to the long-lasting excitation, static components, and softening phenomena. Therefore, almost all wind loading codes/standards, e.g. AIJ-RLB (2004) and ISO4354 (2009), clearly require almost-elastic behavior even for extremely strong wind conditions such as ultimate limit state design. Thus, wind-induced responses of buildings are assumed to be almost-elastic, and the gust loading factor and the equivalent static wind loads in codes/standards are essentially based on linear/elastic structural behavior (ISO 4354, 2009). In this paper, the dynamic behaviors of main frames of buildings are also assumed to be in the elastic region.

As there is no theoretical method for estimating damping in buildings, it is estimated from full-scale data, which shows significant dispersion for various reasons. There are many potential causes of dispersion of full-scale damping data as follows:

- Soil types

†Corresponding author : Yukio Tamura
Tel: +81 (0) 46 242 9547; Fax: +81 (0) 46 242 9547
E-mail: yukio@arch.t-kougei.ac.jp

Table 1. Modal identification methods (Maia & Silva, 1997, He & Fa, 2001, Tamura et al., 2004, 2005)

Time Domain methods		
Least Squares	LS	- FDDR - MDOF curve fitting method
Complex Exponential	CE	- MDOF method in SISO - IRF and complex poles and residues - Sensitive to noise
Least Squares Complex Exponential	LSCE	- MDOF method in SIMO - IRF
Poly-reference Complex Exponential	PRCE	- MDOF method in MIMO - IRF
Ibrahim Time Domain	ITD	- MDOF method in SIMO - Eigenvalue problem from IRF data
Eigensystem Realization Algorithm	ERA	- MDOF method in MIMO - SVD of Markov parameters matrix
Autoregressive Moving Average	ARMA	- MDOF method in SISO - Selection of the optimal order
Direct System Parameter Identification	DSPI	- MDOF method in MIMO - Generalization of CE, PRCE and ITD
Random Decrement	RD	- ACF - SDOF method extracting FDDR
Multi-mode Random Decrement	MRD	- ACF - MDOF method extracting FDDR - LS
Frequency Domain methods		
$\hat{H}_1(\omega)$ model	IFRF	- FRF - No input noise assumption - Cross PSD of input and output & Input Auto PSD
$\hat{H}_2(\omega)$ model	OFRF	- FRF - No output noise assumption - Output Auto PSD & Cross PSD of input and output
$\hat{H}_v(\omega)$ model and $\hat{H}_s(\omega)$ model	VFRF SFRF	- FRF - Both output noise and input noise - LS
Frequency Domain Decomposition	FDD	- PSD matrix - SVD
Hilbert Transform	HT	- FRF - Detecting system non-linearity - No domain change

ACF : Auto-correlation function, MIMO : Multi-input multi-output, FDDR: Free decay damped response, PSD : Power spectral density, FRF : Frequency response function, SIMO : Single-input multi-output, IRF : Impulse response function, SISO : Single-input single-output, MDOF : Multi-degree of freedom, SVD : Singular value decomposition.

- Foundation types
- Structural materials
- Joint types
- Structural frame systems
- Exterior walls
- Interior walls
- Architectural finishing
- Other non-structural members
- Vibration amplitude

These can be taken as parameters for defining the damping value. Although it is very difficult, as shown in Tamura et al. (2000), if full-scale damping data were appropriately categorized based on these parameters, dispersion might be minimized. Thus, these are not necessarily essential sources of dispersion.

On the other hand, ways of obtained damping values can be different depending upon vibration measuring methods, damping evaluation techniques, degree of non-stationarity of excitations, and so on. One of the major reasons for dispersion of full-scale data is inappropriate use of damping evaluation techniques. If a technique is not appropriate, the evaluated damping ratio would be quite different from the true value, as discussed later. However, measurement and evaluation techniques cannot be parameters for the damping value, and if the measurement and evaluation techniques are appropriately chosen and classification of buildings and vibration conditions are efficiently made, the dispersion of the full-scale damping data will be minimized.

This paper reviews past studies of damping in buildings, summarizing our group's works, and comprehensively re-overviews the damping characteristics of buildings. Firstly, it emphasizes the importance of damping evaluation techniques based on field data. Next, it demon-

strates and points out the existence of a critical tip drift ratio showing the maximum damping ratio for a building.

2. Effects of Damping Evaluation Techniques

Many evaluation techniques for modal properties or system identification have been proposed, as shown in Table 1 (Maia and Silva, 1997; He and Fa, 2001; Tamura et al., 2004). The dynamic characteristics of an actual full-scale structure can be obtained by traditional experimental modal analysis techniques. However, these techniques have the following limitations. Artificial excitation or input information is also necessary to measure the Frequency Response Functions (FRFs) or the Impulse Response Functions (IRFs) for subsequent modal parameter extraction. These functions are very difficult to obtain under field conditions and for large structures. Some components, but not a complete system, can be tested in the laboratory environment, but it is not easy to precisely simulate the boundary conditions. Under these situations, Output-Only Modal Estimation (OOME) techniques based on measured responses at a single or multiple points of buildings and structures without any input information are commonly used under field conditions.

3. Quality of Estimated Modal Properties and Points to Note

As discussed, in order to obtain high-quality estimates, it is necessary to conduct careful and high-quality measurements. Test procedures and estimation techniques significantly affect the quality of obtained modal parameters, i.e. natural frequencies, damping ratios, and mode shapes. Ewins (2000) categorized modal test levels as follows:

- Level 0 : Estimation of natural frequencies and damping ratios; response levels measured at a few points; very short test times.
- Level 1 : Estimation of natural frequencies and damping ratios; mode shapes defined qualitatively rather than quantitatively.
- Level 2 : Measurements of all modal parameters suitable for tabulation and mode shape display, albeit un-normalized.
- Level 3 : Measurements of all modal parameters, including normalized mode shapes; full quality checks performed and model usable for model validation.
- Level 4 : Measurements of all modal parameters and residual effects for out-of-range modes; full quality checks performed and model usable for all response-based applications, including modification, coupling and response predictions.

In the building engineering field, chances to conduct full-scale measurements are quite rare, and obtained data are very important and valuable. Therefore, modal parameters obtained by full-scale measurements have been treated as a kind of precious heritage. This is true for natural frequencies and mode shapes obtained under field conditions, which have only 10~20% error. However, low-quality damping data can result in significant errors of 100~200% or even more than 1000%. One of the main reasons is inappropriate frequency resolution, as discussed later. Tests of Level 0 can occasionally have almost no meaning in damping estimations and can provide nonsense results in some cases, especially short term measurements at only a few points for OOME. Furthermore, it cannot be denied that many full-scale data have overestimated damping ratios because of inappropriate measurements and damping estimation methods.

Especially in damping estimations, greater care than Ewins' modal levels (2000) is required to acquire high-quality damping data. Damping estimation techniques obtained from free decay damped response (FDDR), IRF, FRF and ambient vibration data are shown in Table 2. Difficulties and errors in damping evaluation of buildings and structures mainly result from the following:

- Non-stationarity of excitation phenomena and amplitude dependency of damping in buildings
- Non-well-separated modes in terms of natural frequencies
- Local white noise assumption
- Minimal leakage error in PSD estimation
- Sufficient number of ensemble averaging for accurate PSD estimation
- Appropriate width of a band-pass filter for RD technique

Table 2. Damping estimation techniques

Time domain techniques		
Logarithmic decrement	LD	- FDDR - SDOF curve fitting method
Random decrement	RD	- SDOF method extracting FDDR - LD
Multi-mode random decrement	MRD	- MDOF method extracting FDDR - LD
Hilbert transform	HT	- LD - FRF
Frequency domain techniques		
Half power	HP	- Auto-PSD - SDOF
Transfer function	TF	- FRF - SDOF curve fitting method
$1/\sqrt{2}$ Method	$1/\sqrt{2}$	- FRF
Phase gradient	PG	- FRF
Frequency domain decomposition	FDD	- PSD matrix - SVD - Peak Picking
Wavelet transform	WT	- Time-scale decomposition - TRF

- Sufficient number of superimpositions to obtain RD signature

The following sections discuss these items in detail.

3.1. Non-stationarity of excitation phenomena and amplitude dependency of damping in buildings

Seismic excitations are non-stationary and a general building essentially has non-linearity, say amplitude dependency on its dynamic properties, and this always causes difficulty. Wind excitations are rather stationary, but the wind-induced response of a building has fluctuating components, as shown in Figure 1, and amplitude modulation is inevitable, thus requiring careful checking of the amplitude dependency of the dynamic properties. This condition is closely related to the inherent non-linearity of dynamic properties of buildings, shown in Figure 2. This figure shows typical tendencies of dynamic properties of buildings: increasing tendency of damping and decreasing tendency of natural frequency.

As Jeary (1992) pointed out, a mixture of different levels of building responses results in a deformed or broader resonant peak, causing inaccurate estimation of damping ratio. Therefore, stationarity is vital for PSD-based frequency domain techniques, but many papers have reported damping values without checking stationarity of the full-scale records. Stationarity checks such as "run tests" should be made, especially for PSD-based evaluation techniques in the frequency domain. In addition, these papers have not necessarily shown careful checking of the amplitude variation of analyzed data.

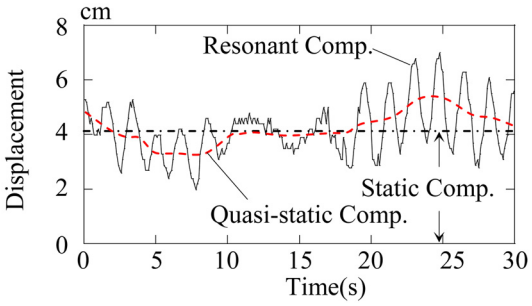

Figure 1. An example of three components of wind-induced response of a structure (Tamura, 2003).

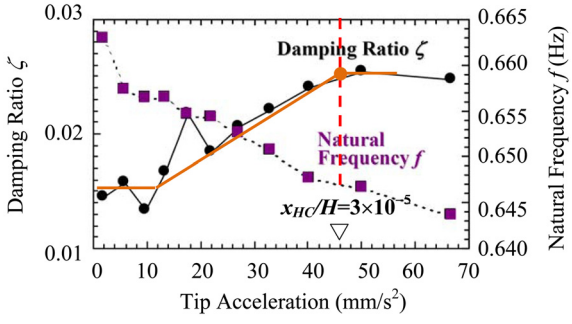

Figure 2. Amplitude dependency of dynamic properties of buildings obtained by RD technique (based on Tamura et al., 1996).

3.2. Non-well-separated modes

These modes always happen with long-span structures. For horizontal vibrations of tall buildings and tower-like structures, natural frequencies of the fundamental mode and higher modes are basically well separated. However, even for these cases, the fundamental natural frequencies, f_x and f_y, of the two translational directions can be very closely located, and their separation is not always easy. This causes difficulty in damping evaluation based on traditional frequency domain techniques such as the Half Power (HP) method and traditional time domain techniques such as the Random Decrement technique. Therefore, items 3.1 and 3.2 are inherent in general buildings and should be carefully taken into account in full-scale vibration measurements and damping evaluation.

The author's group has proposed the Multi-mode Random Decrement (MRD) technique (Tamura et al., 2002, 2005) in the time domain rather than the traditional RD technique (Cole, 1973) to overcome this difficulty. MRD is applicable even for a system having very closely located natural frequencies, and can accurately estimate the amplitude dependency. Figure 3 shows the PSD of ambient accelerations in the y direction at the top of a 220m-high chimney consisting of steel trusses and a concrete funnel, and having an octagonal cross section. Servo-type accelerometers were installed on three different levels. The sampling rate of the acceleration records was set at 100 Hz, and ambient responses were measured for 90 minutes in total. Figure 3(a) shows the PSD of acceleration (y-dir.) at the top of the chimney. Peaks corresponding to several natural frequencies are clearly shown, including a peak near 0.4 Hz. From such a beautifully isolated peak, it is generally easy to estimate the damping ratio, as well as the natural frequency, by the traditional RD technique. Then, the traditional RD technique assuming a SDOF system was applied for system identification using the ambient tip accelerations in the y direction. By processing with a numerical band-pass filter with a frequency range of 0.06~1.0 Hz, only the frequency components around the lowest peak near 0.4 Hz depicted

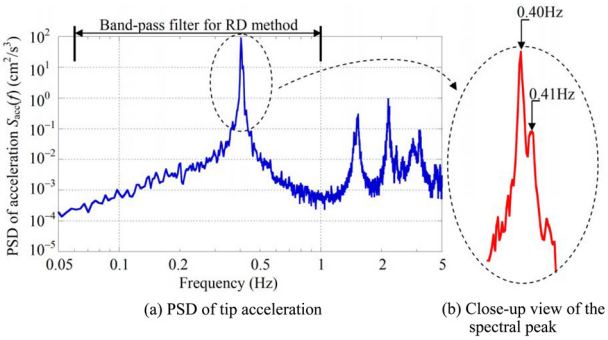

Figure 3. Auto PSD of tip acceleration of 230 m-high chimney.

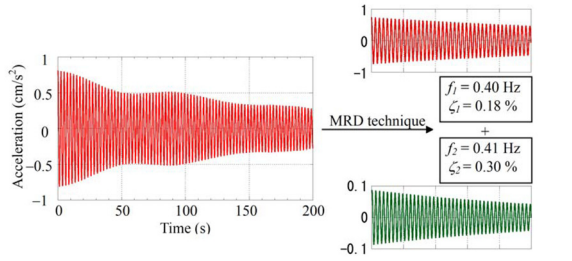

(a) RD signature (b) Two components separated by MRD

Figure 4. RD signature of tip acceleration of 230 m-high chimney and dynamic properties estimated by MRD technique.

in Figure 3(a) were extracted. The initial amplitude of the acceleration to get the RD signature was set at the standard deviation. From the clear peak near 0.4Hz in the PSD shown in Figure 3(a), it was believed that the dynamic property of the first mode would be easily obtained with appropriate accuracy, but this was not correct. Figure 4(a) shows the obtained RD signature, where a beating phenomenon is observed. From such a beating RD signature assuming a SDOF system, it is difficult to get a reliable damping value. However, the beating RD signature suggests two closely located dominant frequency components, and by careful examination of a close-up view of the peak near 0.4 Hz, it is seen that there are actually two peaks: at 0.40 Hz and 0.41 Hz as shown in Figure 3(b). It is of course very difficult to identify whether the peak at 0.41 Hz seen in Figure 3(a) is meaningful or not from PSD due to FFT, and the traditional RD method based on SDOF fails to accurately estimate the damping ratio in such cases. However, the MRD technique proposed by Tamura et al. (2002, 2005) can overcome this shortcoming of the traditional RD method. The MRD technique can separate the beating RD signature shown in Figure 4(a) into the two beautiful RD signatures shown in Figure 4(b). The damping ratio and the natural frequency of the chimney were estimated at 0.18% and 0.40 Hz for the 1st mode, and 0.30% and 0.41 Hz for the 2nd mode. The dynamic characteristics of the 3rd and 4th modes were also estimated by the MRD technique.

For the frequency domain techniques, the author's group has been using the Frequency Domain Decomposition (FDD) technique (Brincker et al., 2000, 2001) based on the Singular Value Decomposition (SVD) of the Power Spectral Density (PSD) matrix, because of its efficiency for systems having closely located natural frequencies. The Singular Value (SV) in the vicinity of the natural frequency is equivalent to the PSD function of the corresponding mode (as a SDOF system). This PSD function is identified around the peak by comparing the mode shape estimate with singular vectors for the frequency lines around the peak. As long as a singular vector is found that has a high Modal Amplitude

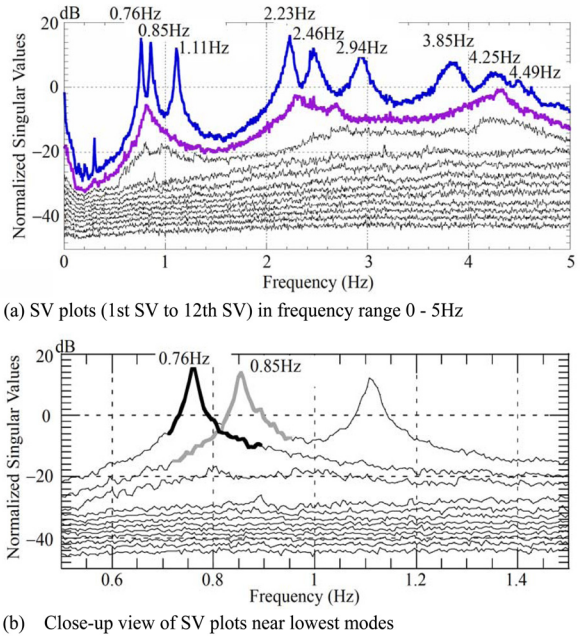

(a) SV plots (1st SV to 12th SV) in frequency range 0 - 5Hz

(b) Close-up view of SV plots near lowest modes

Figure 5. SV plots of 15-story office building.

Coherence (MAC) value with the mode shape, the corresponding SV belongs to the SDOF function. If at a certain line none of the SVs has a singular vector with a MAC value larger than a certain limit value, the search for matching parts of the PSD function is terminated. From the fully or partially identified SDOF PSD function, the natural frequency and the damping ratio can be estimated by taking the PSD function back to the time domain by inverse FFT as an Auto-Correlation Function (ACF) of the SDOF system. From the ACF, the natural frequency and the damping are found by LD or other methods (Brincker et al., 2000, 2001; Tamura et al., 2002, 2005). Figure 5(a) shows the SV plots of the PSD matrix of ambient vibrations of a 15-story steel-framed office building (Tamura et al., 2005; Tamura, 2006). The building extends from 6 m underground to 59 m above basement level. The columns are concrete-filled tubes and the beams are of wide-flange steel. The exterior walls of the first floor are of pre-cast concrete. The walls from the second floor to the top are of ALC. Fourteen servo-type accelerometers were used for one setup with two at the 15th floor as references, and fifty-three components were measured in total. By assuming that the floor was subject to lateral rigid body motion, the measured vibration was translated into equivalent motions at the desired corners. Cross-spectral densities were estimated using the full data of 53 components. In Figure 5(a), there were many peaks of less than 5 Hz corresponding to the natural frequencies, and it was possible to obtain up to the 9th mode below 5 Hz. The lowest two peaks corresponding to 0.76 Hz and 0.85 Hz are closely located. In such situations, the natural frequencies and mode shapes might not be difficult to identify, but damping estimation by using general PSD-

based HP or traditional RD techniques is difficult. However, in the case of FDD, for example, the right-side slope of the first SV peak at 0.76 Hz is smoothly connected to the right slope of the peak of the second SV between 0.76 Hz and 0.85 Hz, as shown in Figure 5(b), which shows a typical "bell" of the SDOF system: the 1st (0.76 Hz) and 2nd (0.85 Hz) modes of the 15-story building. From the identified SDOF spectral density function, the modal frequency and the damping can be estimated by taking the PSD function back to the time domain by inverse FFT as the ACF of the SDOF system. The modal frequency and the damping ratio are found from the ACF.

MRD and FDD can be applied to ambient excitations such as wind, turbulence, traffic, and/or micro-tremors. Many civil engineering structures can be adequately excited by ambient excitations. Ambient modal analysis based on response measurements has two major advantages compared to traditional analysis. One is that no expensive and heavy excitation devices are required. The other is that all (or part) of the measurements can be used as references, and Multi-Input Multi-Output (MIMO) techniques can be used for modal analysis, thus enabling easy handling of closely-spaced and even repeated modes. This is most valuable for long-span roof structures or complex and huge systems such as power transmission line systems. However, each technique should be appropriately used, and misuse of the technique results in significant error in damping estimation.

3.3. Local white noise assumption

Another major cause of errors is inappropriate application of damping evaluation techniques to cases not satisfying the local white-noise assumption. General OOME techniques for damping evaluation such as RD/MRD in the time domain or almost all PSD-based estimation techniques in the frequency domain are not applicable for a narrow-band excitation near the natural frequency such as vortex resonance in crosswind responses of tall buildings. RD/MRD techniques simply derive ACF as an RD signature and treat it as an FDDR to estimate modal parameters including damping ratio (Tamura and suganuma, 1996). ACF becomes exactly the same as FDDR when the excitation is white-noise. Therefore, the excitation should be almost white-noise near the target natural frequency, and vortex resonance is not. Similarly, the shape of the PSD of the building response near the natural frequency can represent the FRF of the system only when the excitation is almost white-noise near the natural frequency. Otherwise, PSD can be too deformed or contaminated to correctly evaluate the damping ratio.

Of course, if the target building is a simple linear SDOF system under a stationary and broad-band excitation, the problems of items 1), 2) and 3) cannot be serious, and there will be no essential difference among the evaluation techniques if they are appropriately applied. Even in such an ideal situation, the damping evaluation should be carefully made, because there are some other points to note for accurate estimation of damping.

3.4. Leakage error in PSD estimation and frequency resolution

This is a serious problem with PSD-based frequency domain techniques. The leakage error of item 4) is due to data truncation of the Discrete Fourier Transform (DFT), which always takes place in practice. This generally results in a larger damping estimation, and occasionally it becomes very large. This has been emphasized by Jeary (1986), Tamura et al. (2002) and others, but many papers have reported unrealistically large damping values without any consideration of this point. Since natural frequencies and mode shapes are not significantly affected by insufficient frequency resolution, people tend to underestimate the importance of this leakage error. This requires a long enough sample for a fine frequency resolution near the target natural frequency.

Figure 6 demonstrates the importance of fine frequency resolution in damping estimation, namely a sufficient length of sample or a sufficient number of DFT data points (Tamura et al., 2004). Figure 6 is the result obtained from laboratory tests on ambient vibrations of a simple four-story lumped-mass model. Damping ratios were obtained by the various frequency domain estimation methods, where the Auto PSDs or FRF was calculated via DFT. The abscissa indicates the number of data points used for DFT calculation. The evaluated damping ratios decrease with increasing number of DFT data points and converge to a constant value around 0.25%, which was thought to be the accurate damping value. If the number of DFT was set at only 1024, as the fundamental estimation of PSD by FFT often does, the evaluated damping ratio can be 3%, which is more than 10 times the accurate damping value, say accompanying a 1000% error. Leakage is a kind of bias error, which cannot be eliminated by windowing, e.g. by applying a Hanning window, and is harmful to the damping estimation accuracy, which relies on the PSD measurements. The bias error caused by leakage is proportional to the square of the frequency resolution (Bendat and Piersol, 1986). Therefore, increasing the frequency resolution is a

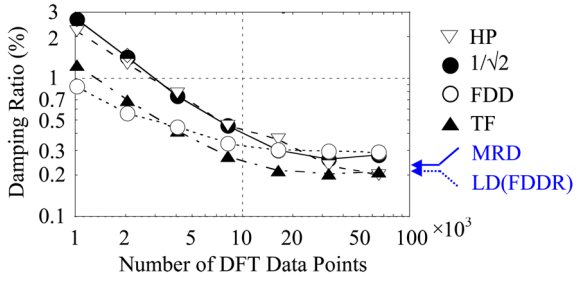

Figure 6. Variations of damping ratios evaluated by PSD based frequency domain techniques with DFT data points demonstrating leakage effects.

very effective way to reduce leakage error. It is always necessary to check the convergence of the damping value due to increase of the number of DFT.

3.5. Sufficient number of ensemble averaging for accurate PSD estimation

This is related to accurate estimation of the PSD of the response, which basically requires enough ensemble averaging. A full-scale measurement of the response is assumed to be made for a total length of T_T in a stationary condition, and then the record is divided into N stationary samples with a sample length of $T_s = T_T/N$. In order to minimize the leakage error described in 3.4, the sample length T_s should be large enough, which means N should be small. However, in order to have enough ensemble averaging, the number of samples N should be large. This creates difficulties in field testing, but to satisfy the conditions required by items 3.4 and 3.5, the total length T_T should be sufficiently large. This is a must to get accurate and reliable damping data.

3.6. Appropriate width of a band-pass filter

For time domain techniques such as RD techniques, appropriate selection of the band-width of the band-pass filter is required to extract a target natural frequency component. An appropriate band-pass-filter width is required to get a good RD signature targeting a particular mode from full-scale data of the MDOF system, and an appropriate band-pass filter is required to extract the frequency component only around the target natural frequency, in the case of the traditional RD technique. A too-narrow band-pass filter provides a smaller damping ratio than the true value, and a too-wide band-pass filter gives a RD signature contaminated by other frequency components. However, if the neighboring natural frequencies are closely located, it is almost impossible to extract the target mode component appropriately. For such a case, the MRD proposed by Tamura et al. (2002, 2005) is appropriate, as shown in Figures 3 and 4.

3.7. Sufficient number of superimpositions to get RD signature

This is also required to get a good RD signature that well represents FDDR, and requires a long full-scale record. The error ratio of the RD signature to the theoretical FDDR fitted by the LS method can be a useful index for accurate damping evaluation. The author's group adopts an estimated damping ratio with an error ratio less than 3%.

In summary, in order to obtain reliable and accurate damping values from full-scale records by OOME techniques, a long enough record is required when the vibration measurements are conducted. Table 3 summarizes the important points and necessary conditions to be satis-

Table 3. Points to note for evaluation of damping in buildings using ambient vibrations (OOME)

Techniques	Required Conditions	Measures
Time Domain - RD - MRD	- Sufficient number of superimpositions	- Long enough data - Error ratio (< 3%) based on theoretical SDOF FDDR
	- Appropriate bandwidth of band-pass filter (not too narrow and wide enough)	- Sufficient number of superimpositions - Application of MRD
	- Local white-noise assumption	- Careful check of excitation condition*[1]
	- Well-separated modes	- Application of MRD
Frequency Domain - HP - FDD	- Stationarity	- Run tests
	- Fine frequency resolution (Minimal leakage error)	- Convergence check of damping ratio by increasing sample length - Long enough data
	- Sufficient ensemble averaging of PSD	- High quality PSD - Long enough data
	- Local white-noise assumption	- Careful check of excitation condition*[1]
	- Well-separated modes	- Application of FDD
Other necessary information	- Amplitude information	- Tip drift ratio x_H/H - Initial amplitude (RD/MRD)
	- Building information	- Height and stories - Plan shape and dimensions - Material of structural frames - Structural type - Building usage - Type of foundation - Soil condition - Cladding type
	- Measurement/Excitation information	- Excitation type - Length of samples

*1 A narrowband excitation near the target natural frequency such as vortex resonance is inappropriate.

fied in damping evaluation. The damping data should be evaluated and reported considering these points. 1000% error cannot be treated as a minor error, but should be accepted as a major mistake. It should be noted that no data is much better than such wrong and contaminated data, and it is very important to carefully examine the available damping data and to have the courage to reject it if it is 2, 10 or more times larger than the true value, even if almost no other data are available.

4. General Tendency of Damping in Buildings and Structures

4.1. Viscous damping assumption and stick-slip model

It is well known that a structure can be damped by mechanisms with different internal and external characteristics: friction between atomic/molecular or different parts, impact, air/fluid resistance, and so on. Combinations of different phenomena result in various types of damping. In structural dynamics, damping is described by viscous, hysteretic, coulomb or velocity-squared models. Viscous damping occurs when the damping force is proportional to the velocity, and is mathematically convenient because it results in a linear second order differential equation for engineering structures. Fortunately, damping in buildings can be approximated by the viscous damping formula even if there is no viscous material in it.

The most realistic model for the physical external friction damping mechanism for built-up structures was evolved by Wyatt (1977) and is expressed by the "STICTION" term, which is randomly distributed with respect to amplitude. STICTION represents a STuck frICTION element, in which a contact surface between members does not move in the very low amplitude range, but begins to slip at a particular amplitude, thus losing its stiffness (Jeary, 1986) as shown in Figure 7 (Tamura, 2006).

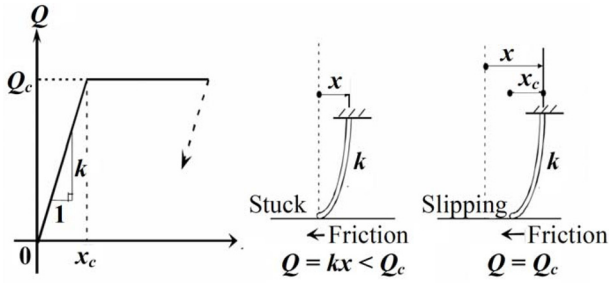

Figure 7. Stick-slip model for damping in buildings (Tamura, 2006).

The number of slipping contact surfaces increases with amplitude, so the damping due to friction increases as the natural frequency decreases. This is expressed by the term "Stick-Slip" in Davenport and Hill-Carroll (1986). The contribution of non-load-bearing secondary members to building stiffness is suggested by the variation of natural frequency with amplitude, shown in Figure 2 (and Figures 10, 12, and 13 shown later), and also understood by Figure 8. Figure 8 shows the difference between the measured and design values of natural periods based on the Japanese Damping Database (Tamura et al., 2000, Tamura, 2003, Satake et al., 2003) for steel buildings. Measurements were basically made under low-amplitude conditions, in which almost all contact surfaces were stuck and the secondary members contributed to stiffness. On the other hand, the design values were estimated based on FEM models considering only main frames, and it is difficult to include the contributions of secondary members. Consequently, the design natural periods are 20% higher than the measured values, as shown in Figure 8. Almost the same results were obtained for reinforced concrete buildings.

The integrated effect of a lot of different friction damping elements causes the building to respond as if it were equipped with a linear viscous damping system, as shown

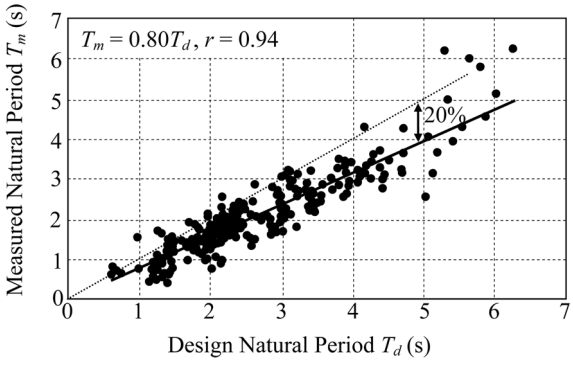

Figure 8. Suggestion of contribution of non-load-bearing members to stiffness (Tamura et al., 2000).

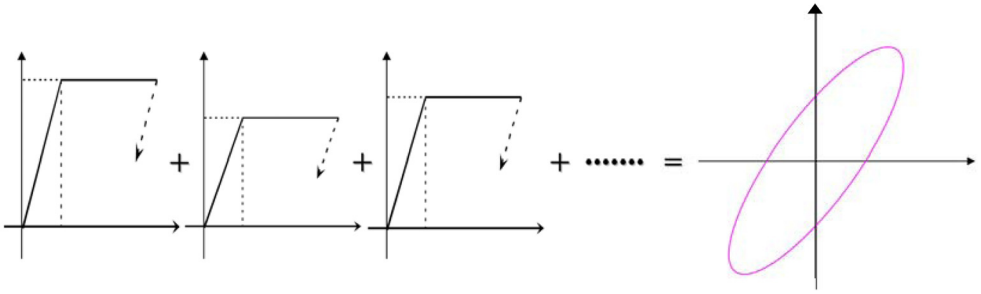

Figure 9. Viscous damping model as integration of numerous friction damping components.

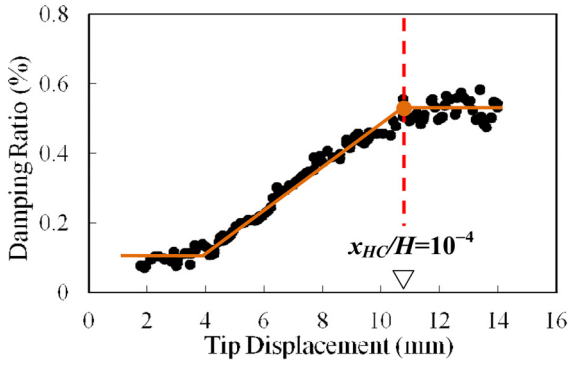

Figure 10. Amplitude dependency of damping ratio of a 100 m-high steel building (based on Jeary, 1998).

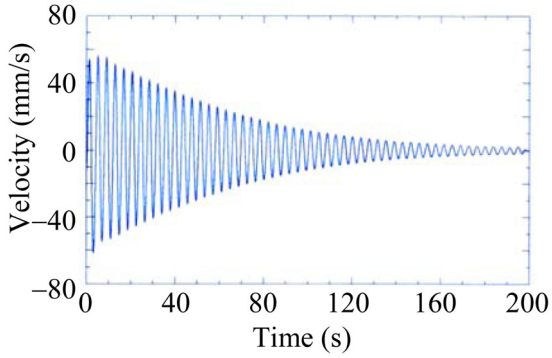

Figure 11. FDDR of 200 m-high office building after sudden stop of HMD (Okada et al., 1993).

in Figure 9. From a practical point of view, equivalent viscous damping, which models the overall damping behaviour of a structural system as being viscous, is often adopted in structural dynamics and is thought to be appropriate.

4.2. Variation of damping ratio with amplitude

Figure 2 shows a typical amplitude dependency of dynamic properties obtained by the RD technique (Tamura et al., 2000). The building is a steel-framed observatory tower 99.35 m high. It has a 16.5 m-square cross section in its lower third, a 12.1 m-square cross section in its middle third and an octagonal section in its upper third. The reinforced concrete foundation is supported by caisson-type piles. The exterior walls are made of glass-fiber-reinforced concrete panels (Tamura and Suganuma, 1996). It is clearly demonstrated that the fundamental natural frequency decreases and the damping ratio decreases with acceleration amplitude. These tendencies are understood by the stick-slip model explained in 4.1.

Another example is the 100 m-high steel building (Jeary, 1998) shown in Figure 10. Jeary (1998) pointed out the following three parts: a low-amplitude plateau, a mid-amplitude slope, and a high-amplitude plateau. It should be noted that the mid-amplitude slope where the damping ratio increases with amplitude ends at a relatively small amplitude level of around 11 mm in terms of the tip displacement, x_H. As the building height H is 100 m, the tip drift ratio x_H/H is only around 10^{-4}. Although Jeary (1998) did not mention it, Figure 10 implies that damping ratio does not necessarily increase at higher amplitude levels beyond the amplitude range shown in the figure.

Figure 2 also shows the same tendency, where the abscissa indicates the tip acceleration amplitude (Tamura et al., 2000). The increasing tendency ends at around a_H = 46 mm/s^2. Considering the natural frequency around f_1 = 0.66 Hz, the tip displacement is roughly estimated by x_H $a_H/(2\pi f_1)^2$ as 3 mm. Thus, the tip drift ratio x_H/H is only 3×10^{-5}, which is also very small. Here, the tip drift ratio where the damping increasing tendency ends is defined as "critical tip drift ratio" in this paper. It should also be noted that the damping ratio at the high-amplitude plateau seems to begin to decrease in Figures 2 and 10. The damping ratio does not increase any more with amplitude in the amplitude range above the critical tip drift ratio.

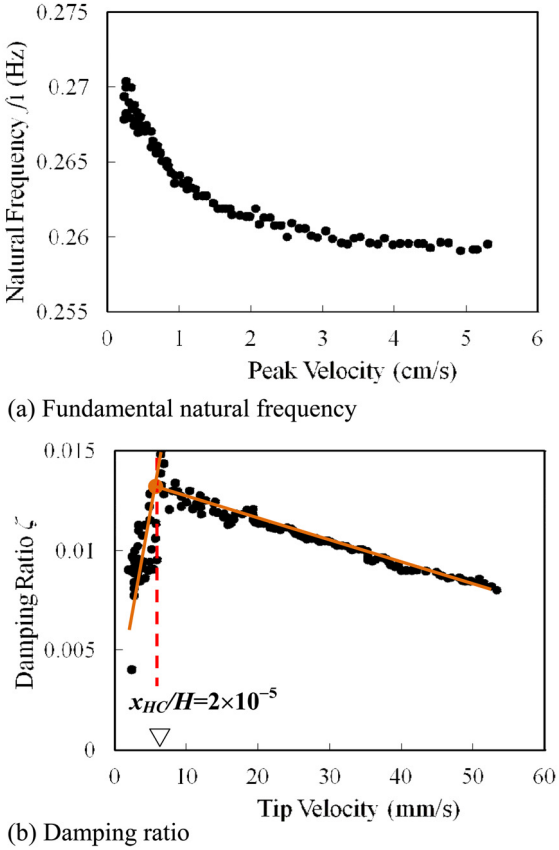

Figure 12. Variation of fundamental natural frequency and damping ratio of a 200 m-high steel-framed office building (Step by step evaluation from FDDR, based on Okada et al., 1993).

There is another interesting result obtained for a 200 m-high steel-framed office building with a Hybrid Mass Damper (HMD) installed at its top. Before occupation of this building, the HMD was used as an exciter, and relatively large amplitude vibration tests were conducted

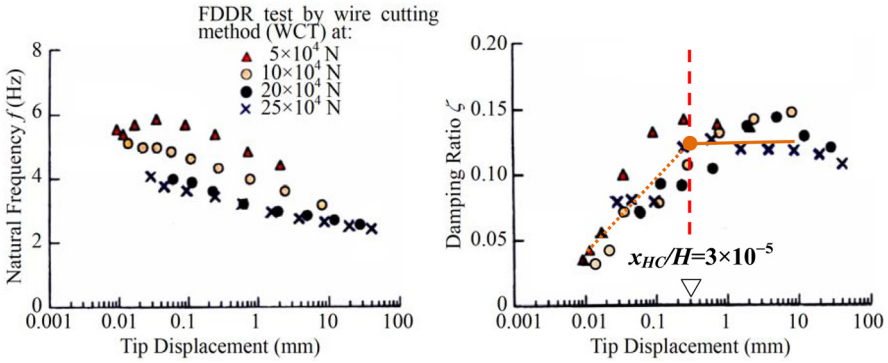

(a) Natural frequency (b) Damping ratio

Figure 13. Variations of fundamental natural frequency and damping ratio of a 3-story building with amplitude (based on Fukuwa et al., 1996).

(Okada et al., 1993). Figure 11 shows an example of an FDDR after a sudden stop of excitation by the HMD. From this beautiful damped-free oscillation record, step-by-step evaluations of damping ratio and natural frequency were made (Okada et al., 1993). Obtained fundamental natural frequency and damping ratio are shown in Figures 12(a) and 12(b) (after Okada et al., 1993). The fundamental natural frequency, f_1 0.26 Hz, decreases with velocity amplitude and saturates at around 30 mm/s. The damping ratio increases in the low-amplitude regime, and reaches its maximum at around the response velocity v_H = 6 mm/s. Thus, the tip displacement $x_H \approx v_H/(2\pi f_1)$ is roughly estimated at 4 mm. The critical tip drift ratio is estimated at $x_H/H = 2 \times 10^{-5}$, which is also very small. In the higher amplitude regime greater than this critical drift ratio, the damping ratio clearly decreases with amplitude.

The previous example showed valuable data of relatively large amplitude. There is insufficient data on damping ratio at very high amplitudes within the elastic limit of main frames, and it is difficult to show general characteristics of dynamic properties in a very high amplitude regime. However, an example of dynamic characteristics at a very high amplitude is shown in Figures 13(a) and 13(b) (Fukuwa et al., 1996), in which tendencies similar to Figure 2 are recognized in the natural frequency and damping ratio. The building is a three-story steel-framed experimental house with autoclaved lightweight concrete (ALC) panel slabs, ALC panel exterior walls, and plaster board partitions. The ALC panel exterior walls, with a thickness of 100 mm, do not provide shear stiffness under horizontal loads. They are connected to the frames at their tops, permitting only a rocking type movement, although silicone sealing compounds fill the gaps between panels. This exterior wall system contributes significantly to structural damping, so it cannot be said that the results demonstrate typical dynamic characteristics of buildings. As the building height is only about 10m, the effect of the soil-structure interaction (SSI) is very significant. Additionally, excitation was made up to 4×10^{-3} in terms of tip drift ratio, and the maximum acceleration was almost 1,000 milli-g. The maximum amplitude was large enough to damage the plaster board partitions, and cracks appeared not only in the ALC slabs but also in the ALC exterior walls.

Under these conditions, the estimated damping ratio was large. However, it reached a maximum value at around 0.3 mm tip displacement. Thus, the "critical tip drift ratio" is estimated at 3×10^{-5}(Figure 13(b)), which is consistent with the previous results in Figures 2 and 10. Even after the damping ratio reached its maximum value with increasing amplitude, the natural frequency still decreased, as shown in Figures 2, 12(a) and 13(a). This is also reasonable, because the damping ratio can decrease even when the number of slipping contact surfaces increases, thus reducing the stiffness, if the increasing rate of amplitude is more significant than that of the number of slipping contact surfaces.

Here, it should be noted that the damping ratio never increases in a higher amplitude regime exceeding the "critical tip drift ratio" unless there are additional sources of damping forces. As explained above, there is a possibility of damage to secondary members such as non-load-bearing walls, interior partitions, slabs, and architectural finishings in the large-amplitude range. However, if those kinds of damage are not allowed in allowable-stress-level design, as in many current codes, a high damping ratio cannot be expected even near the elastic limit of frames. Considering the decreasing tendency demonstrated by Okada et al. (1993), it is assumed that the maximum damping ratio in Figure 13(b) was maintained because of the non-linear effect of SSI of a low-rise building and damage to partitions, non-load-bearing ALC exterior walls and ALC slabs observed at a high-amplitude level such as 1G acceleration response, while the main frames remained within the elastic limit.

4.3. Critical tip drift ratio

The critical value of tip drift ratio representing the maximum damping ratio in the non-damaged situation has been defined as "critical tip drift ratio" in this paper.

Table 4. Critical tip drift ratio

Buildings	Frame	Height: H (m)	Critical tip drift ratio: x_{HC}/H
Observatory building	Steel	99	3×10^{-5}
Office building	Steel	100	1×10^{-4}
Office building	Steel	200	2×10^{-5}
Residential house	Steel	10	3×10^{-5}

Table 4 summarizes the critical tip drift ratios, x_{HC}/H, obtained for the four buildings. It is very interesting that those ratios for buildings with heights ranging from 10 m to 200 m show similar values ranging from 2×10^{-5} to 1×10^{-4}. Although it is dangerous make a general conclusion, we should note that the damping ratio of a building does not necessarily increase with amplitude continuously, but reaches its maximum at a very low amplitude level.

4.4. Decrease of damping with amplitude

One example shown in Figure 12(b) clearly indicates and all other examples slightly suggest a "decreasing tendency" of damping at the higher amplitude level. The reason for this is not difficult to understand. As already mentioned, increasing amplitude increases the number of slipping contact surfaces, and the damping ratio increases with amplitude. However, after reaching an amplitude where all contact surfaces slip, the total friction force at the slipping contact surfaces causing friction damping does not increase any more with amplitude, i.e., the total friction force remains constant with increasing amplitude. For a simple forced vibration system with a constant damping force F, i.e. Coulomb damping, a steady state amplitude A and a circular natural frequency w, the equivalent viscous damping coefficient C can be simply expressed as Eq. (1):

$$C = \frac{4F}{\pi A \omega} \tag{1}$$

The equivalent damping ratio ζ is given as Eq. (2):

$$\zeta = \frac{C}{2M\omega_0} = \frac{2F}{\pi A M \omega \omega_0} \tag{2}$$

Thus, if the friction damping force F is constant, the "damping ratio" decreases with increasing amplitude A. There has been a misunderstanding that the damping ratio increases with amplitude. However, that is not correct. It decreases with amplitude from the "critical tip drift ratio", which is very small, being in the order of 10^{-5} to 10^{-4}.

4.5. Design value recommendations

High-quality damping data from 285 buildings were collected by a research committee of the Architectural Institute of Japan (AIJ) (see Tamura et al., 2000; Satake et al., 2003). This committee conducted surveys on damping data from relatively new literature and from 40 collaborative organizations. Based on the Japanese Damping Database, empirical formulae of natural frequencies were derived as follows (Eqs. (3) and (4)):

$$f_1 = \begin{cases} \dfrac{1}{0.015H} = \dfrac{67}{H} & \text{(For Habitability Level)} \quad (3a) \\ \dfrac{1}{0.018H} = \dfrac{56}{H} & \text{(For Safety Level)} \quad (3b) \end{cases}$$

: RC Buildings

$$f_1 = \begin{cases} \dfrac{1}{0.020H} = \dfrac{50}{H} & \text{(For Habitability Level)} \quad (4a) \\ \dfrac{1}{0.024H} = \dfrac{42}{H} & \text{(For safety Level)} \quad (4b) \end{cases}$$

: Steel Buildings

For higher and torsional modes, Tamura et al. (2000) reported linear relations of natural frequencies such as $f_2 = 3.05f_1$, $f_3 = 5.46f_1$, $f_4 = 7.69f_1$, and $f_T = 1.34f_1$, with very high correlation coefficients, namely 99%, 95%, 91% and 94%, for steel buildings. Therefore, the natural frequencies of higher and torsional modes of steel buildings can be expressed as functions of building height H as follows:

$$f_2 = \begin{cases} \dfrac{150}{H} & \text{(For habitability Level)} \quad (4c) \\ \dfrac{130}{H} & \text{(For Safety Level)} \quad (4d) \end{cases}$$

: Steel Buildings

$$f_3 = \begin{cases} \dfrac{270}{H} & \text{(For habitability Level)} \\ \dfrac{230}{H} & \text{(For Safety Level)} \end{cases} \quad (4e)$$

: Steel Buildings

$$f_4 = \begin{cases} \dfrac{380}{H} & \text{(For habitability Level)} \\ \dfrac{320}{H} & \text{(For Safety Level)} \end{cases} \quad (4f)$$

: Steel Buildings

$$f_T = \begin{cases} \dfrac{67}{H} & \text{(For habitability Level)} \quad (4g) \\ \dfrac{56}{H} & \text{(For Safety Level)} \quad (4h) \end{cases}$$

: Steel Buildings

Tamura et al. (2000) also proposed damping predictors as empirical regression equations within the range of tip drift ratio $x_H/H \le 2 \times 10^{-5}$ for building heights in the range of 10 m < H < 100 m for RC buildings and 30 m < H < 200 m for steel buildings as follows (Eqs. (5) and (6)).

$$\zeta_1 = 0.014f_1 + 470\frac{x_H}{H} - 0.0018 \quad \text{: RC Buildings} \tag{5}$$

$$\zeta_1 = 0.013f_1 + 400\frac{x_H}{H} - 0.0029 \quad \text{: Steel Buildings} \tag{6}$$

These predictors consist of a natural-frequency-dependent term, an amplitude-dependent term and a correction term. However, there is no clear reason for the frequency effects, and the natural-frequency-dependent term does not actually express the effect of vibration frequency, but may be attributed to the effect of SSI. A low-rise building with a high natural frequency makes a significant contribution to the SSI effect. Thus, it tends to have higher total damping. Therefore, considering the relations between the natural frequency and the building height given in Eqs. (3a) and (4a), the frequency-dependent term is replaced by a height-dependent term. Finally, the damping predictors are given as follows (Eqs. (7) and (8)):

$$\zeta_1 = \frac{0.93}{H} + 470\frac{x_H}{H} - 0.0018 \quad : \text{RC Buildings} \tag{7}$$

$$\zeta_1 = \frac{0.65}{H} + 400\frac{x_H}{H} + 0.0029 \quad : \text{Steel Buildings} \tag{8}$$

The predictors obtained from Eqs. (7) and (8) are believed to be reliable, and the correlation coefficient of the damping values predicted by Eq. (7) and the full-scale values whose amplitudes are known, for example, was 88% (Tamura et al., 2000).

However, it should be noted that the scope of application of the above empirical formulae, Eqs. (7) and (8) as damping estimates for building design is limited to the amplitude range $x_H/H \le 2 \times 10^{-5}$, and there is no guarantee of an increasing tendency in a higher amplitude range. Considering the dispersion of the data, the following 20%-lower values (Eqs. (9) and (10)) are recommended for wind-resistant design of office buildings:

$$\zeta_1 = \frac{0.75}{H} + 380\frac{x_H}{H} - 0.0014 \quad : \text{RC Buildings} \tag{9}$$

$$\zeta_1 = \frac{0.52}{H} + 320\frac{x_H}{H} + 0.0023 \quad : \text{Steel Buildings} \tag{10}$$

Based on the Japanese Damping Database, the first mode damping ratios of office buildings having few interior walls and hotels and apartment buildings having many interior walls are compared. The average damping ratios are obtained as follows (Eqs. (11) and (12)):

$$\zeta_1 = 0.0115 \tag{11}$$

: Office Buildings (Average Building height $H = 113$ m)

$$\zeta_1 = 0.0145 \tag{12}$$

: Hotels and Apartment Buildings (Average Building height $H = 100$ m)

The results suggest that almost 25% larger damping ratios are obtained for hotels and apartment buildings with many interior walls. Therefore, Eqs. (5) and (6) may be applicable for wind-resistant design of hotels and apartment buildings.

For higher-mode damping, the ratios of mode damping values such as z_2/z_1 and z_3/z_2 were examined based on the Japanese Damping Database (Tamura et al., 2000), and average values were obtained as follows (Eqs. (13) and (14)):

$$\frac{\zeta_{n+1}}{\zeta_n} = 1.4 \quad : \text{RC Buildings} \tag{13}$$

$$\frac{\zeta_{n+1}}{\zeta_n} = 1.3 \quad : \text{Steel Buildings} \tag{14}$$

for $n = 1$ and 2. On average, 30% to 40% larger damping ratios were obtained for the next higher mode.

However, it is noteworthy that the above relations do not imply stiffness-proportional damping characteristics, which is often assumed in structural design. It is also important that some data suggest higher mode reducing damping ratios for medium-rise and low-rise buildings, and the scope of application of Eqs. (13) and (14) should be limited to tall buildings.

5. Concluding Remarks

This paper has discussed some important points regarding vibration measurements and techniques for evaluating damping in buildings, as well as general characteristics of damping in buildings including amplitude dependency. The following facts were clarified.

Only full-scale damping data carefully evaluated considering Table 3 should be adopted as reliable data, and we should have the courage to exclude low-quality data without necessary consideration or information shown in Table 3.

The critical tip drift ratio, at which damping ratio stops increasing with amplitude, was defined. The critical tip drift ratio was around 10^{-5} to 10^{-4}. Damping ratio tends to decrease at higher amplitudes, unless there is no damage to secondary members and architectural finishing.

For wind-resistant design within allowable stress levels, namely in the elastic range of main structural frames, we should realize the fact that there is no guarantee of increasing tendency of damping above the critical drift ratio. Therefore, it should be emphasized that the recommended damping ratio expressed by Eqs. (7)~(10) should be used.

Acknowledgements

The author has been studying damping in buildings for almost two decades with many colleagues, and wishes to extend his gratitude to all of them for their kind and keen collaborations. The author's special thanks should be given to Dr. Akihito Yoshida from Tokyo Polytechnic University, Prof. Lingmi Zhang from Nanjing University of Aeronautics and Astronautics for their long-term collaborations. The author also thanks Mr. Ronwaldo Emmanuel Aquino and Dr. Yong Chul Kim for their support in preparation of this manuscript. Finally, the author is grateful for financial support by

the Ministry of Education, Culture, Sports, Science and Technology, Japanese Government, by way of Global Center of Excellent Program from 2008.

References

AIJ RLB (2004) Recommendation for loads on buildings, Architectural Institute of Japan, Maruzen.

Bendat, J. and Piersol, A. (1986) Random data analysis and measurement procedures, John ‘Wiley & Son, New York, USA.

Brincker, R., Zhang, L. M., and Anderson, P. (2000) “Modal identification from ambient response using frequency domain decomposition”, *Proc. 18th International Modal Analysis Conference* (*IMAC*).

Brincker, R., Ventura, C. E., and Andersen, P. (2001) “Damping estimation by frequency domain decomposition”, *Proc. 19th International Modal Analysis Conference* (*IMAC*).

Cole, H. A. (1973) “On-line failure detection and damping measurement of aerospace structures by the random decrement signatures”, NASA CR-2205.

Davenport, A. G. and Hill-Carroll, P. (1986) “Damping in tall buildings: Its variability and treatment in design, Building Motion in Wind” *Proc. ASCE Spring Convention*, Seattle, Washington, pp. 42~57.

Ewins, D. J. (2000) “Modal testing, theory, practice and applications”, 2nd Ed., Research Studies Press Ltd., England.

Fukuwa, N., Nishizawa, R., Yagi, S., Tanaka, K., and Tamura, Y. (1996) “Field measurement of damping and natural frequency of an actual steel-framed building over a wide range of amplitude”, *Journal of Wind Engineering and Industrial Aerodynamics*, 59, pp. 325~347.

Havilland, R. (1976) “A study of the uncertainties in the fundamental translational periods and damping values for real buildings”, Massachusetts Institute of Technology, PB-253, pp. 188.

He, J. M. and Fu, Z. F. (2001) Modal analysis, Butterworth-Heinemann, USA.

ISO4354 (2009) Wind actions on structures, International Standard.

Jeary, A. P. (1986) “Damping in buildings - a mechanism and a predictor”, *Journal of Earthquake Engineering and Structural Dynamics*, 14, pp. 733~750.

Jeary, A. P. (1992) “Establishing non-linear damping characteristics of structures from non-stationary response time-histories”, *The Structural Engineer*, 70(4), pp. 61-66.

Jeary, A. P. (1998) “The damping parameter as a descriptor of energy release in structures”, *Proc. CD-ROM, T193-4, Structural Engineers World Congress*, San Francisco, 8.

Maia, N. M. M. and Silva, J. M. M. (1997) Theoretical and experimental modal analysis, Research Studies Press, Ltd., England.

Okada, K., Nakamura, Y., Shiba, K., Hayakawa, T., Tsuji, E., Ukita, T., and Yamaura, N. (1993) “Forced vibration tests of ORC200 Symbol Tower, Part 1 Test methods and results”, *Summaries of Technical Papers of Annual Meeting of Architectural Institute of Japan*, Structures 1, pp. 875~876.

Satake, N., Suda, K., Arakawa, T., Sasaki, A., and Tamura, Y. (2003) “Damping evaluation using full-scale data of buildings in Japan”, *Journal of Structural Engineering*, ASCE, April, pp. 470~477.

Tamura, Y. and Suganuma, S. (1996) “Evaluation of amplitude-dependent damping and natural frequency of buildings during strong winds”, *Journal of Wind Engineering and Industrial Aerodynamics*, 59, pp. 115~130.

Tamura, Y., Suda, K., and Sasaki, A. (2000) “Damping in buildings for wind resistant design”, *Proc. International Symposium on Wind and Structures for the 21st Century*, Cheju, Korea, pp. 115~130.

Tamura, Y., Yasui H., and Marukawa, H. (2001) “Non-elastic responses of tall steel buildings subjected to across-wind forces”, *Wind and Structures*, 4(2), pp. 147~162.

Tamura, Y., Zhang, L.-M., Yoshida, A., Nakata, S., and Itoh, T. (2002) “Ambient vibration tests and modal identification of structures by FDD and 2DOF-RD technique”, *Structural Engineers World Congress* (*SEWC*), Yokohama, Japan, T1-1-a-1, pp. 8.

Tamura, Y. (2003) “Design issues for tall buildings from accelerations to damping -Tribute to Hatsuo Ishizaki and Vinod Modi-”, *Proc. 11th International Conference on Wind Engineering*, INV.W2, Lubbock, Texas, USA, pp. 81~114.

Tamura, Y., Yoshida, A., and Zhang, L. (2004) “Evaluation techniques for damping in buildings”, *International Workshop on Wind Engineering & Science*, New Delhi.

Tamura, Y., Yoshida, A., and Zhang, L. (2005) “Damping in buildings and estimation techniques”, *Proc. 6th Asia-Pacific Conference on Wind Engineering* (*APCWE-VI*), Seoul, Korea, pp. 193~214.

Tamura, Y. (2006) “Amplitude dependency of damping in buildings and estimation techniques”, *Proc. 12th Australasian Wind Engineering Society Workshop*, Queenstown, New Zealand.

Tamura, Y. (2009) “Wind and tall buildings”, *Proc. 5th European and African Conference on Wind Engineering*, Florence, Italy.

Tsujita, O., Hayabe, Y., and Ohkuma, T. (1997) “A study on wind-induced response for inelastic structure”, *Proc. ICOSSAR’97*, pp. 1359~1366.

Wyatt, T. A. (1977) “Mechanisms of damping.” *Proc. Symposium on dynamic behaviour of bridges*, Transport and Road Research Laboratory, Crowthorne, Berkshire.